

The halo of the exotic nucleus ^{11}Li : a single Cooper pair

F. Barranco¹, R. A. Broglia^{2,3,4}, G. Colo^{2,3}, E. Vigezzi^{2,3}

¹Escuela de Ingenieros Industriales,

Universidad de Sevilla, Camino de los Descubrimientos, 41092 Seville, Spain

²Department of Physics, University of Milan, Via Celoria 16, 20133, Milan, Italy

³INFN, Sezione di Milano, Milan, Italy

⁴The Niels Bohr Institute, University of Copenhagen,

Blegdamsvej 17, 2100 Copenhagen, Denmark

If neutrons are progressively added to a normal nucleus, the Pauli principle forces them into states of higher momentum. When the core becomes neutron-saturated, the nucleus expels most of the wavefunction of the last neutrons outside to form a halo, which because of its large size can have lower momentum. It is an open question how nature stabilizes such a fragile system and provides the glue needed to bind the halo neutrons to the core. Here we show that this problem is similar to that of the instability of the normal state of an electron system at zero temperature solved by Cooper, solution which is at the basis of BCS theory of superconductivity. By mimicking this approach using, aside from the bare nucleon-nucleon interaction, the long wavelength vibrations of the nucleus ^{11}Li , the paradigm of halo nuclei, as tailored glues of the least bound neutrons, we are able to obtain a unified and quantitative picture of the observed properties of ^{11}Li .

Aside from “dark matter” [1], atomic nuclei, little droplets made out of protons and neutrons 10 femtometer across [2], make up a sizable fraction of the present mass of the universe. Research into the structure of atomic nuclei concentrates largely on the limits of the nuclear stability [3], where new physics is expected to be, in particular at the limits of neutron and proton number defining the so called drip lines in the chart of nuclides. The most exotic nuclei [4], first produced in the laboratory only few years ago, are those that lie just within the drip lines, on the edges of nuclear stability. Of these, the atomic nucleus $^{11}_{3}\text{Li}_8$, containing 3 protons and 8 neutrons, is rightly the most famous and better studied and provides the cleanest example of halo nuclei to date [5–11].

In halo nuclei, some of the constituent neutrons or protons venture beyond the drop’s surface and form a misty cloud or halo. Not surprisingly, these extended nuclei behave very differently from ordinary (“normal”) nuclei lying along the so-called stability valley in the chart of nuclides. In particular, they are larger than normal nuclei of the same mass number, and they interact with them with larger cross sections as well. In the case of ^{11}Li , the last two neutrons are very weakly bound. Consequently, these neutrons need very little energy to move away from the nucleus. There they can remain in their “stratospheric” orbits, spreading out and forming a tenuous halo. If one neutron is taken away from ^{11}Li , a second neutron will come out immediately, leaving behind the core of the system, the ordinary nucleus ^9Li . This result testifies to the fact that pairing, the attraction correlating pairs between the least bound particles in a system, plays a central role in the stability of ^{11}Li .

It is well known that pairing can radically affect the properties of a many-body system. In metals, pairing between the electrons gives rise to superconductivity [12]. In a dilute neutron gas, pairing can influence the properties of neutron stars, cold remnants of fierce supernova explosions [13]. Acting on a liquid made out of atoms of the lighter isotope of helium ($^3_2\text{He}_1$) it leads to superfluidity [14]. In nuclei, it controls almost every aspect of nuclear structure close to the ground state and determines, to a large extent, which nuclei are stable and which are not [2,15].

The basic experimental facts which characterize ^{11}Li and which are also of particular

relevance in connection with pairing in this system are: a) $^9_3\text{Li}_6$ and $^{11}_3\text{Li}_8$ are stable, $^{10}_3\text{Li}_7$ is not, b) the two-neutron separation energy in ^{11}Li is only $S_{2n}=0.294\pm0.03$ MeV [7] as compared with values of 10 to 30 MeV in stable nuclei, c) ^{10}Li displays s- and p-wave resonances at low energy, their centroids lying within the energy range 0.1-0.25 MeV and 0.5-0.6 MeV respectively [16], d) the mean square radius of ^{11}Li , $\langle r^2 \rangle^{1/2}=3.55\pm 0.10$ fm [17-19], is very large as compared to the value 2.32 ± 0.02 fm of the ^9Li core, and testifies to the fact that the neutron halo must have a large radius ($\approx 6-7$ fm), e) the momentum distribution of the halo neutrons is found to be exceedingly narrow, its FWHM being equal to $\sigma_{\perp} = 48\pm 10$ MeV/c for the (perpendicular) distribution observed in the case of the break up of ^{11}Li on ^{12}C , a value which is of the order of one fifth of that measured during the break up of normal nuclei [6,7], f) the ground state of ^{11}Li is a mixture of configurations where the two halo nucleons move around the ^9Li core in s^2- and p^2- configurations with almost equal weight [20,21].

Before discussing the sources of pairing correlations in ^{11}Li , we shall study the single-particle resonant spectrum of ^{10}Li . The basis of (bare) single-particle states used was determined by calculating the eigenvalues and eigenfunctions of a nucleon moving in a Saxon-Woods potential with spin-orbit and symmetry term (cf. [2], Vol. I, Eqs. (2.281) and (2.282)). The continuum states of this potential were calculated by solving the problem in a box of radius equal to 40 fm, chosen so as to make the results associated with ^{10}Li and ^{11}Li discussed below, stable. While mean field theory predicts the orbital $p_{1/2}$ to be lower than the $s_{1/2}$ orbital (cf. Fig. 1, I(a)), experimentally the situation is reversed. Similar parity inversions have been observed in other isotones of $^{10}_3\text{Li}_7$, like e.g. $^{11}_4\text{Be}_7$. Shell model calculations testify to the fact that the effect of core excitation, in particular of quadrupole type, play a central role in this inversion [22],(cf. also [23]). In keeping with this result, we have studied the effect the coupling of the $p_{1/2}$ and $s_{1/2}$ orbitals of ^{10}Li to monopole-, dipole- and quadrupole-vibrations of the ^9Li core has on the properties of the $1/2^+$ and $1/2^-$ states of this system. In this study we have used vibrational states calculated by diagonalizing, in the random phase approximation (RPA), a multipole-multipole separable interaction

taking into account the contributions arising from the excitation of particles into the continuum states. The coupling strengths were adjusted so as to reproduce the position and transition probabilities of vibrational states in the normal nucleus ^{10}Be [24]. Unperturbed particle-hole excitations up to 70 MeV have been included in the calculations and phonon states up to 50 MeV have been considered. Within this space there are of the order of 10^2 dipole states and about the same amount of quadrupole states, exhausting the associated energy-weighted sum rules. The resulting vibrational states were coupled to the particle states making use of the associated transition densities (formfactors) and particle-vibration coupling strengths. A Skyrme-type effective interaction (SLy4) was used to calculate the monopole linear response. The corresponding solutions were obtained in coordinate space making use of a mesh extending up to a radius of 80 fm. The monopole response exhausts 94% of the EWSR considering the summed contributions up to 40 MeV of excitation energy. This response function was discretized in bins of 300 keV and the resulting states coupled to the single-particle states making use of the corresponding transition densities and particle-vibration coupling strengths. Similar calculations were performed to determine the properties of the $L=0,1$ and 2-vibrational states of ^{11}Li needed in connection with the discussion of the pairing induced interaction carried out below. In this case the strength of the separable dipole interactions has been slightly changed from the value used in the previous calculation so as to provide an overall account of the experimental dipole response in ^{11}Li [25,26]. For the quadrupole strength the same value used before was employed. Because the calculations have been carried out on the physical (correlated) ^{11}Li ground state, the transitions associated with the vibrational states involving the $p_{1/2}$ and the $s_{1/2}$ states have been renormalized with the corresponding occupation numbers resulting from the full diagonalization.

In the study of the single-particle resonances of ^{10}Li we have considered not only the particle-vibration coupling vertices associated with effective-mass-like diagrams (upper-part graph of Fig. 1, I(b)) and leading to attractive (negative) contributions to the single-particle energies, but also those couplings leading to Pauli principle (repulsive) correction

processes associated with diagrams containing two-particles, one-hole and a vibration in the intermediate states (lower-part diagram of Fig. 1, I(b)). Because of such Pauli correction processes, the $p_{1/2}$ state experiences an upward shift in energy, arising from the coupling of this orbital to the $p_{3/2}$ hole-state through quadrupole vibrational states, in keeping with the fact that the $(p_{1/2}p_{3/2}^{-1})$ particle-hole excitation constitutes an important component of the quadrupole vibration wavefunction. As a consequence, the $p_{1/2}$ state becomes unbound, turning into a low-lying resonance with centroid $E_{res} \approx 0.5$ MeV. Due to the coupling to the vibrations the s -states are instead shifted downwards. In fact, in this case there are essentially no (repulsive) contributions arising from the Pauli correction processes. On the other hand, (attractive) effective-mass-like processes with intermediate states consisting of one particle plus a vibrational state of the type $(s_{1/2} \times 0^+)$, $(p_{1/2} \times 1^-)$ and $(d_{5/2} \times 2^+)$ lead to a virtual state with $E_{virt} = 0.2$ MeV (cf. Fig. 1, I(b)), the coupling to quadrupole vibrations providing by far the largest contribution to the total energy shift. The important difference between the distribution of the single-particle strength associated with the resonant state $p_{1/2}$ and the virtual state $s_{1/2}$ can be observed in Fig. 1, I(c), where the partial cross section σ_l for neutron elastic scattering off ${}^9\text{Li}$ is shown. While σ_p displays a clear peak at 0.5 MeV, σ_s is a smoothly decreasing function of the energy. On the other hand, a small increase in the depth of the potential felt by the s -neutron will lead to a (slightly) bound state, hence the name of virtual [27].

At the basis of the variety of pairing phenomena observed in systems so apparently different as atomic nuclei and metals is the formation of Cooper pairs [28,29]. In the case of metals, Cooper pairs arise from the combined effect of Pauli principle and of the exchange of lattice vibrations (phonons) between pairs of electrons (fermions) moving in time reversal states lying close to the Fermi energy. In the superconducting or BCS state of metals [12], Cooper pairs are strongly overlapping. In fact, there are on average 10^6 pairs which have their centers of mass falling within the extent of a given pair wavefunction. In spite of the modest number of Cooper pairs present in the ground state of atomic nuclei (≤ 10), BCS theory gives a quite accurate description of pairing in nuclei [2,30], the analogy between

the pairing gap typical of metallic superconductors and of atomic nuclei being very much to the point [31]. On the other hand, the finiteness of the nucleus introduces in the BCS treatment of pairing important modifications (quantal size effects (QSE), [30], [32]- [34]). In particular, while in the infinite system the existence of a bound state of the (Cooper) pair happens for an arbitrarily weak interaction [28], in the nuclear case this phenomenon takes place only if the strength of the nucleon-nucleon potential is larger than a critical value connected with the discreteness of the nuclear spectrum. In fact, calculations carried out making use of a particularly successful parametrization of the (bare) potential (Argonne potential [35]), testify to the fact that the nuclear forces are able to bind Cooper pairs in open shell nuclei (leading to sizable pairing gaps (1-2 MeV) [37]), but not in closed shell nuclei, the most important contributions to the nucleon-nucleon (pairing) interaction arising from high multipole components of the force [30].

The situation is however quite different for the "open shell" nucleus ^{11}Li . In fact, allowing the two neutrons to interact through the Argonne potential produces almost no mixing between s - and p -waves, but essentially it only shifts the energy of the unperturbed (resonant) states $s_{1/2}^2(0)$ and $p_{1/2}^2(0)$ by about 80 keV without giving rise to a bound system. Similarly, making use of the matrix elements of the same nucleon-nucleon potential in connection with the BCS equations does not lead to a solution but the trivial one of zero pairing gap ($\Delta_\nu = 0, U_\nu V_\nu = 0$) [30]. At the basis of this negative result is the fact that the most important single-particle states allowed to the halo neutrons of ^{11}Li to correlate are the $s_{1/2}$, $p_{1/2}$ and $d_{5/2}$ orbitals. Consequently the two neutrons are not able, in this low-angular momentum phase space, to profit fully from the strong force-pairing interaction, as only the components of multipolarity $L = 0, 1$ and 2 of this force are effective in ^{11}Li because of angular momentum and parity conservation [38].

In keeping with this result and with those of ref. [42], and making use of the fact that ^{11}Li displays low-lying collective vibrations [25,26], one can posit that the exchange of these vibrations between the two neutrons is the main source of pairing available to them to correlate. In fact, allowing the two neutrons to both exchange phonons (induced interaction,

Fig. 1, II(a)), as well as to emit and later reabsorb them (self-energy correction, Fig. 1, I(b)), leads to a bound (Cooper) pair, the lowest eigenstate of the associated secular matrix being $E_{gs} = -0.270$ MeV. Adding to the induced interaction the nucleon-nucleon Argonne potential one obtains $E_{gs} = -0.330$ MeV, and thus a two-neutron separation energy quite close to the experimental value. Measured from the unperturbed energy of a pair of neutrons in the lowest state calculated for ^{10}Li , namely the s -resonance ($E_{unp} = 2E_{s_{1/2}} = 400$ keV, cf. Fig. 1,I(b)), it leads to a pairing correlation energy $E_o = E_{unp} - E_{g.s.} = 0.730$ MeV (cf. Fig. 1, II(b)). From the associated two-particle ground state wavefunction $\Psi_0(\vec{r}_1, \vec{r}_2) (\equiv \langle \vec{r}_1, \vec{r}_2 | 0^+ \rangle)$, one obtains a momentum distribution (whose FWHM is $\sigma_\perp = 56$ MeV/c, for ^{11}Li on ^{12}C) and ground state occupation probabilities of the two-particle states $s_{1/2}^2(0)$, $p_{1/2}^2(0)$ and $d_{5/2}^2(0)$ (0.40, 0.58 and 0.02 respectively, cf. Fig. 1,II(b)) which provide an overall account of the experimental findings. The radius of the associated single-particle distribution is 7.1 fm. Adding to this density that of the core nucleons one obtains the total density of ^{11}Li . The associated mean square radius (3.9 fm) is slightly larger than the experimental value.

The spatial structure of the Cooper pair described by the wavefunction $\Psi_0(\vec{r}_1, \vec{r}_2)$ is displayed in Fig. 2. The mean square radius of the center of mass of the two neutrons is $\langle r_{cm}^2 \rangle^{1/2} = 5.4$ fm. This result testifies to the importance the correlations have in collecting the small (enhanced) amplitudes of the uncorrelated two-particle configuration $s_{1/2}^2(0)$ in the region between 4 to 5 fm, region in which the $p_{1/2}^2(0)$, helped by the centrifugal barrier, displays a somewhat larger concentration (Fig. 3). From the above results, it emerges that the exchange of vibrations between the least bound neutrons leads to a (density-dependent) pairing interaction acting essentially only outside the core (cf. also ref. [43]). To be noted that the long wavelength behaviour of these vibrations is connected with the excitation of the neutron halo, the large size of which not only makes the system easily polarizable but provides also the elastic medium through which the loosely bound neutrons exchange vibrations with each other [44].

The average mean square distance between the halo neutrons is $\langle r_{12}^2 \rangle^{1/2} \approx 9.2$ fm, in keeping with the fact that the coherence length [12] associated with Cooper pairs in nuclei is

larger than the nuclear dimensions thus preventing the possibility of a nuclear supercurrent (cf. e.g. [2] Vol. II, p. 398). On the other hand, this value of $\langle r_{12}^2 \rangle$ does not prevent the two correlated neutrons to be close together. The corresponding (small) probability (cf. Fig. 2) being much larger than that associated with the uncorrelated neutrons (cf. Fig. 3).

Similar results as those reported above are obtained solving the BCS equation for the two-neutron system making use of the matrix elements used in the diagonalization, sum of those of the nucleon-nucleon Argonne potential and those of the induced interaction. In this case, the correlation energy is $E_o = 0.7$ MeV, the separation energy of the two neutrons becoming $S_{2n} = 0.3$ MeV. The radial structure of the projected BCS wavefunctions $\sum_{\nu>0} (V_{\nu}/U_{\nu}) \varphi_{\nu}(\vec{r}_1) \varphi_{\nu}(\vec{r}_2)$ displays a spatial structure quite similar to $\Psi_0(\vec{r}_1, \vec{r}_2)$, the admixture of s-, p- and d- two particle configurations being now 46% and 51% and 3% respectively. The coherence length ξ , that is the mean square distance between the two neutrons forming the Cooper pair, is in this case, $\langle r_{12}^2 \rangle^{1/2} = 7.8$ fm.

Arguably, the understanding of halo nuclei is the single, most important issue of nuclear structure research still awaiting a satisfactory explanation. We have shown that a substantial advance towards this goal is made by properly characterizing the role the surface of the system plays in renormalizing the bare nucleon-nucleon potential and the single-particle motion of the nucleons. In fact, we find compelling evidence which testifies to the fact that the mechanism which is at the basis of the presence of a low density halo in ^{11}Li , is the coupling of weakly bound nucleons to long wavelength vibrations of the system leading to pairing instability and thus to a bound system. This result suggests a general strategy for designing nuclei with a large excess of neutrons or protons which may prove valuable in the current exploration of the drip line of the chart of nuclides, and thus in the design of new nucleon species: select those systems which display, under an increase of the excess of one type of nucleons, a marked softening of the long wavelength linear response. It is likely that such systems could venture far inside the region delimited by the drip lines, in keeping with the fact that the associated vibrational modes are expected to be an important source of (induced) pairing interaction, and thus to contribute significantly to the stability of the

system.

We wish to thank G. Gori for technical help.

Correspondence and request for materials should be addressed to RAB (e-mail: broglia@mi.infn.it)

- [1] J.A. Peacock, *Cosmological Physics*, Cambridge University Press, Cambridge (1999).
- [2] A. Bohr and B.R. Mottelson, *Nuclear Structure*, Vol. I and II, Benjamin, Reading, Massachusetts (1969,1975).
- [3] Y.T. Oganessian et al., *Nature* **400** (1999) 242.
- [4] *Exotic Nuclei*, 4th Course, International School of Heavy Ion Physics, Eds. R. A. Broglia and P. G. Hansen, World Scientific, Singapore (1998).
- [5] P. G. Hansen, A. S. Jensen, B. Jonson, *Annu. Rev. Nucl. Part. Sci.* **45** (1995) 591.
- [6] T. Kobayashi, *et al.*, *Nucl. Phys.* **A553** (1993) 465.
- [7] I. Tanihata, *J. Phys. G* **22** (1996) 157.
- [8] R. Anne et al., *Phys. Lett.* **B250** (1990) 19.
- [9] E. Arnold et al., *Phys. Lett.* **B281** (1992) 16.
- [10] H. Esbensen and G.F. Bertsch, *Nucl. Phys.* **A542** (1992) 310.
- [11] F. Barranco, E. Vigezzi, R.A. Broglia, *Z. Phys. A* **356** (1996) 45.
- [12] J. R. Schrieffer, *Theory of Superconductivity*, Benjamin, New York (1964).
- [13] *The structure and evolution of neutron stars*, eds. D. Pines, R. Tamagaki and S. Tsuruta, Addison-Wesley, Menlo Park, California (1992).

[14] A. Leggett, in *The New Physics*, Ed. P. Davies, Cambridge University Press, Cambridge (1989), pag. 268.

[15] P. Walker, G. Dracoulis, *Nature* **399** (1999) 35.

[16] M. Zinser et al., *Phys. Rev. Lett.* **75** (1995) 1719.

[17] T. Kobayashi et al., *Phys. Lett.* **B232** (1989) 51.

[18] J.S. Al-Khalili, J.A. Tostevin, *Phys. Rev. Lett.* **76** (1996) 3903.

[19] P. G. Hansen, *Nature* **384** (1996) 413.

[20] N. Aoi et al., *Nucl. Phys.* **A616** (1997) 181c.

[21] H. Simon et al., *Phys. Rev. Lett.* **83** (1999) 496.

[22] H. Sagawa, B. A. Brown, H. Esbensen, *Phys. Rev. Lett.* **B309** (1993) 1.

[23] N. Vinh Mau, *Nucl. Phys.* **A592** (1995) 33.

[24] F. Ajzenberg-Selove, *Nucl. Phys.* **A490**(1988)1

[25] D. Sackett et al., *Phys. Rev.* **C48**(1993)118.

[26] M. Zinser et al., *Nucl. Phys.* **A619** (1997) 151.

[27] L. Landau and E. Lifshits, *Quantum Mechanics*, Pergamon Press, par. 133.

[28] L.N. Cooper, *Phys. Rev.* **104** (1956) 1189.

[29] J. Bardeen, L.N. Cooper, and J.R. Schrieffer, *Phys. Rev.* **106**(1957) 162; **108** (1957) 1175.

[30] S.T. Belyaev, *Mat. Fys. Medd. Dan. Vid. Selsk.* **31** no. 11 (1959).

[31] A. Bohr, B.R. Mottelson and D. Pines, *Phys. Rev.* **110** (1958)936.

[32] R. Kubo, *J. Phys. Soc. Jap.* **17**(1962)975.

[33] R.H. Parmenter, *Phys. Rev.* **166**(1968)2490.

[34] P.W. Anderson, J. Phys. Chem. Solids **11**(1959)26.

[35] This nucleon-nucleon potential has been designed [36] so as to accurately reproduce the nucleon-nucleon phase shifts.

[36] R.B. Wiringa, R.A. Smith and T.L. Ainsworth, Phys. Rev. **C29**(1984)1207.

[37] F. Barranco, R.A. Broglia, H. Esbensen, E. Vigezzi, Phys. Lett. **B390** (1996)13

[38] This is the reason why the Cooper pair problem and the BCS treatment of pairing in the case of ^{11}Li looks (qualitatively) different from pairing in nuclei lying along the stability valley, and more similar to pairing in metals [12], [28], or even better in doped fullerides [39]- [41].

[39] C.M. Lieber, Z. Zhang, Sol. State Phys. **48**(1994)349; W. Pickett, *ibid.*, p. 266.

[40] M. Cotè et al., Phys. Rev. Lett. **81**(1998)697.

[41] N. Breda, R.A. Broglia, G. Colò, D. Provati, G. Onida, E. Vigezzi, Phys. Rev. **B**, in press.

[42] F. Barranco, R. A. Broglia, G. Gori, E. Vigezzi, P. F. Bortignon, J. Terasaki, Phys. Rev. Lett. **83** (1999) 2147.

[43] G.F. Bertsch and H. Esbensen, Ann. Phys. **209**(1991)327.

[44] In keeping with the fact that the vibrational states of ^{11}Li are built out of excitations which occupy, to some extent, the same particle states occupied by the loosely bound neutrons we are studying, the corresponding particle-vibration matrix elements have been corrected from Pauli violating contributions. In particular, the reduction factors aassociated with the matrix elements $\langle s_{1/2} \times 1^- | H_c | p_{1/2} \rangle$, $\langle s_{1/2} \times 0^+ | H_c | s_{1/2} \rangle$ and $\langle p_{1/2} \times 0^+ | H_c | p_{1/2} \rangle$ of the particle-vibration coupling Hamiltonian H_c the reduction factor are 0.68, 0.25 and 0.25 respectively.

Caption to the figures

Fig. 1

(I) **Single-particle neutron resonances in ^{10}Li .** In (a) the position of the levels $s_{1/2}$ and $p_{1/2}$ calculated making use of mean field theory is shown (hatched area and thin horizontal line respectively). The coupling of a single-neutron (upward pointing arrowed line) to a vibration (wavy line) calculated making use of the Feynman diagrams displayed in (b) (schematically depicted also in terms of either solid dots (neutron) or open circles (neutron hole) moving in a single-particle level around or in the ^9Li core (hatched area)), leads to conspicuous shifts in the energy centroid of the $s_{1/2}$ and $p_{1/2}$ resonances (shown by thick horizontal lines) and eventually to an inversion in their sequence. In (c) we show the calculated partial cross section σ_l for neutron elastic scattering off ^9Li .

(II) **The two-neutron system ^{11}Li .** We show in (a) the mean-field picture of ^{11}Li , where two neutrons (solid dots) move in time-reversal states around the core ^9Li (hatched area) in the $s_{1/2}$ resonance leading to an unbound $s_{1/2}^2(0)$ state where the two neutrons are coupled to zero angular momentum. The exchange of vibrations between the two neutrons shown in the upper part of the figure leads to a density dependent interaction which, added to the nucleon-nucleon interaction, correlates the two-neutron system leading to a bound state $|0^+\rangle$, where the two neutrons move with probability 0.40, 0.58 and 0.02 in the two-particle configurations $s_{1/2}^2(0)$, $p_{1/2}^2(0)$ and $d_{5/2}^2(0)$ respectively.

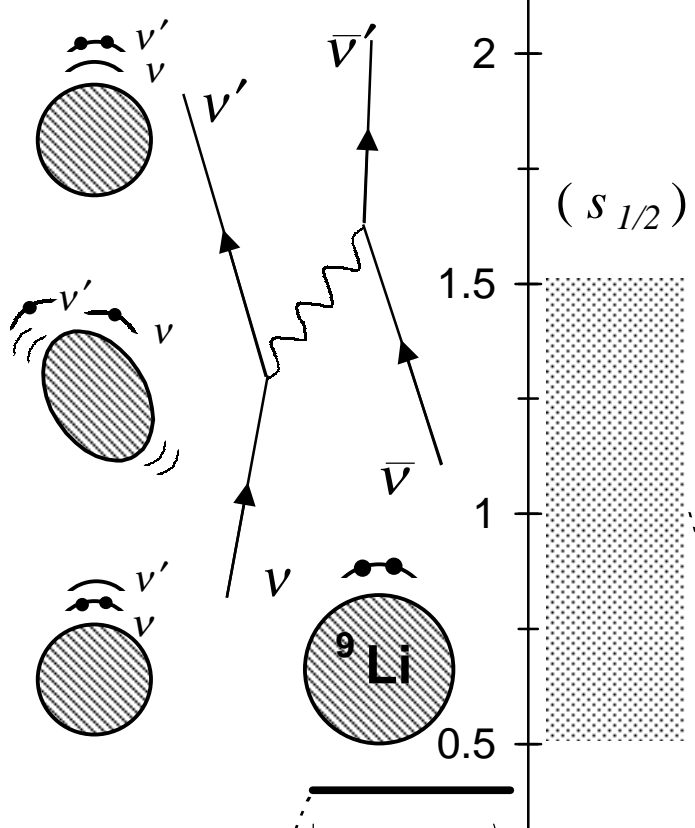
Fig. 2

Spatial structure of two-neutron Cooper pair. The modulus squared wavefunction $|\Psi_0(\vec{r}_1, \vec{r}_2)|^2 = |\langle \vec{r}_1, \vec{r}_2 | 0^+ \rangle|^2$ (cf. Fig. 1, II (b)) describing the motion of the two halo neutrons around the ^9Li core (normalized to unity and multiplied by $16\pi^2 r_1^2 r_2^2$) is displayed as a function of the cartesian coordinates $x_2 = r_2 \cos(\theta_{12})$ and $y_2 = r_2 \sin(\theta_{12})$ of particle 2, for fixed value of the position of particle 1 ($r_1 = 2.5, 5, 7.5$ fm) represented in the right panels by a solid dot, while the core ^9Li is shown as a red circle. The numbers appearing on the z -axis of the three-dimensional plots displayed on the left side of the figure are in units of

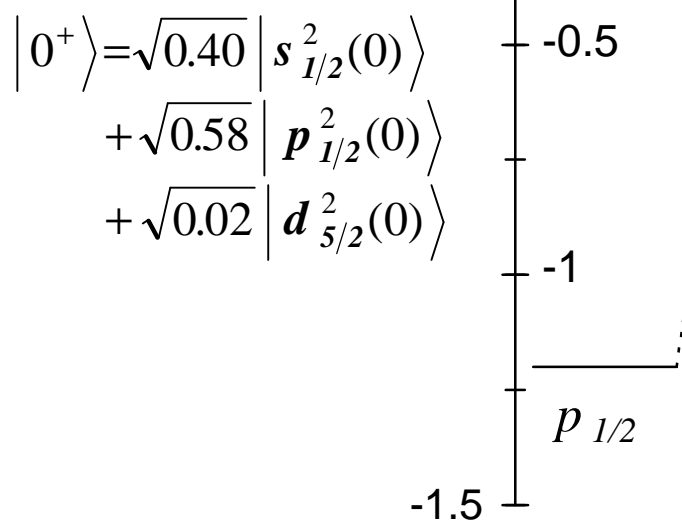
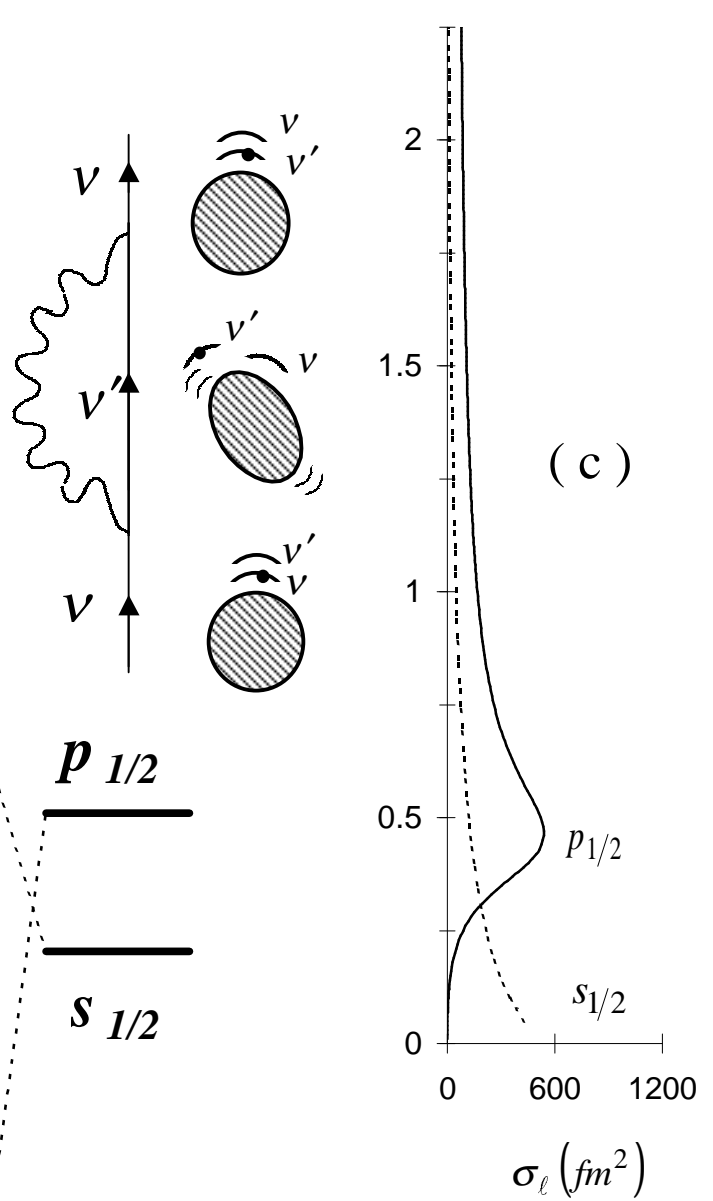
fm^{-2} .

Fig. 3 Spatial distribution of the pure two-particle configurations $s_{1/2}^2(0)$ and $p_{1/2}^2(0)$ as a function of the x - and y -coordinates of particle 2, for a fixed value of the coordinate of particle 1 ($r_1=5$ fm). For more details cf. caption to Fig. 2.

(II)



(I)



(b)

(a)

(a)

(b)